Slow dynamics and aging of a confined granular flow

G. Ovarlez and E. Clément
Laboratoire des Milieux Désordonnés et Hétérogènes, UMR 7603, Université Pierre et Marie Curie, Boîte 86, 4 Place Jussieu, F-75252 Paris, France
(Received 25 February 2003; published 3 September 2003)

We present experimental results on slow flow properties of a granular assembly confined in a vertical column and driven upwards at a constant velocity V. The wall roughness is much lower than the typical grain size. For monodisperse assemblies this study evidences at low velocities ($1<V<100$ μm/s) a stiffening behavior, i.e., the stress necessary to obtain a steady-state velocity increases roughly logarithmically with velocity. On the other hand, at very low driving velocity ($V<1$ μm/s), we evidence a discontinuous and hysteretic transition to a stick-slip regime characterized by a strong divergence of the maximal blockage force when the velocity goes to zero. We show that all this phenomenology is strongly influenced by surrounding humidity. We also present an attempt to establish a link between the granular rheology and the solid friction forces between the wall and the grains. We base our discussions on a simple theoretical model and independent grain/wall tribology measurements. We also use finite element numerical simulations to compare experimental results with isotropic elasticity. A second system made of polydisperse assemblies of glass beads is investigated. We emphasize the onset of a new dynamical behavior, i.e., the large distribution of blockage forces evidenced in the stick-slip regime.

DOI: 10.1103/PhysRevE.68.031302 PACS number(s): 45.70.−n, 46.55.+d, 81.05.Rm

I. INTRODUCTION

Granular flows are presently the focus of many attentions [1]. The classical model for granular media stability was proposed at the end of the 18th century by de Coulomb who revealed a strong analogy between the failure properties of a granular assembly and the phenomenology of solid-on-solid friction. Modern developments have elaborated sophisticated empirical approaches around this fundamental idea [2], but so far there is no deep physical understanding or rigorous derivation describing the passage from the granular level description to a set of evolution equations involving macroscopic quantities such as stress, strain, or packing fraction. Furthermore, there is an additional difficulty to understand complex behaviors such as aging under stress or to account for the influence of external parameters such as surrounding humidity, the effects of which are often observed in practice. Note that similar questions are still under active consideration in the field of tribology [3–5], but in the case of granular assemblies, a supplementary difficulty lies in the fragile character of granular structures which can be easily modified under the action of external constraints.

Actually, recent aging experiments in granular media [6,7] found logarithmic aging of static friction enhanced by an increase in relative humidity. These results have been interpreted by the dynamics of capillary condensation at the contacts [6,8]. However, aging is also observed for a granular material immersed [9], where capillary condensation cannot occur, under the condition that the material is sheared during aging. Solid-on-solid experiments also reveal logarithmic aging of static friction enhanced by an increase in relative humidity [4], but there may be other sources of aging of static friction: creep of contacts [3] or chemical reactions at the interface [9]. A very recent solid-on-solid experiment [5] shows that relative humidity may also have an influence on dynamic friction.

The dynamical behavior of a slider has been deeply investigated by Heslot *et al.* [10]. They found that for low driving velocity, the dynamical coefficient of friction decreases with velocity (this is the velocity weakening regime), whereas it may increase with velocity for higher driving velocities (this is the velocity strengthening regime). In the velocity weakening regime, a continuous transition to stick-slip motion may occur when decreasing the driving velocity. In the velocity strengthening regime, the transition to stick-slip motion is a finite amplitude, hysteretic transition.

Dynamical behavior of slowly driven granular materials was investigated by different groups both in compression and/or in shearing experiments [9,11–13]. Plane shearing experiments [9,13] reveal stick-slip motion at low velocity, but the origin of this dynamical regime remains unclear in the case of granular materials: the relevant length scale is the grain scale in Ref. [9], whereas it may be the roughness scale in Ref. [13].

Here we present an experimental situation of the same type, but in a quite different geometry. We investigate the rheology of a granular assembly confined in a cylindrical column and pushed it vertically from the bottom. The resistance to vertical motion as well as the blocking/unblocking transitions reveals a phenomenology possibly shared by many confined granular assemblies. Note that this column configuration may help us to understand several practical situations such as pipe flows [14], compaction under stress, or dense granular paste extrusion. A previous investigation with the same display was made in two dimensions (2D) [15] and also in 3D [16] as a preliminary report, and for recent experiments see Refs. [17,18]. These contributions have shown a rich phenomenology partly sorted by the solid friction properties of the grains and the boundaries. The importance of surrounding humidity was also evidenced [16] as it would strongly influence the rheology of the granular column. In this paper, we push further the investigation as we

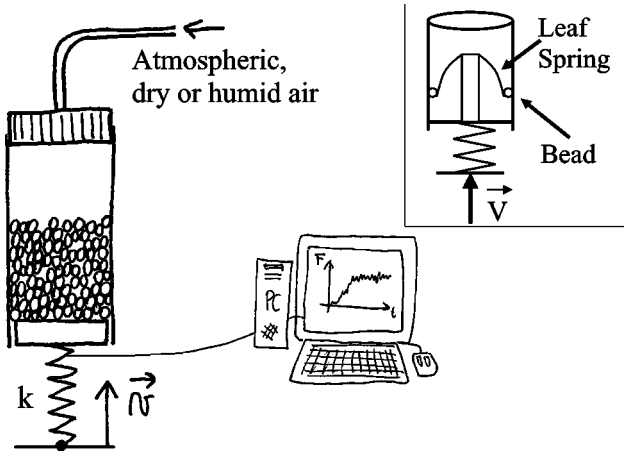

FIG. 1. Sketch of the experimental setup. Inset: sketch of the slider.

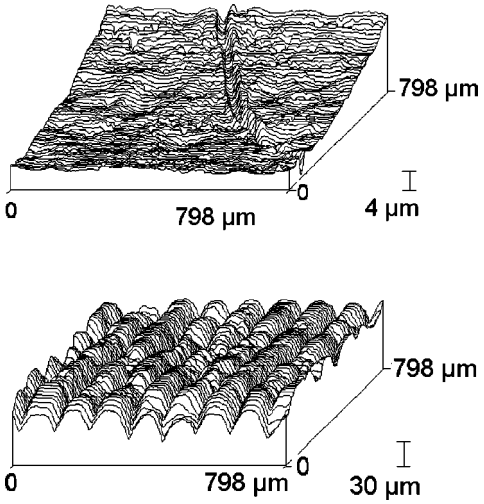

FIG. 2. Topographies [21] of internal surfaces of duralumin (top image) and brass (bottom image) columns used in our experiments. The surfaces were scanned on 800 μm by 800 μm, with 2 μm steps; vertical resolution is 100 nm. The horizontal axis on the graphs is the symmetry axis of the columns.

change the column material, the beads characteristics and size dispersity, under various humidity conditions. We also propose to compare our data with the outcome of a simple numerical model of isotropic elasticity.

In the classical situation of Newtonian fluid pushed by a piston (typically in a syringe), one would obtain a relation between pressure and flow rate, which is characterized by a fluid constitutive parameter: the viscosity. For an isotropic elastic medium, the resistance to pushing would depend on the material's Poisson ratio and wall frictional properties [19,20] (we will discuss this question further in the text). For a granular material, the situation is *a priori* more complex since the piling structure can be modified so as to adapt to the external constraints. Friction at the walls may also create internal granular recirculation flows [15]. Therefore it is an important but difficult matter to clarify the rheology of this system by sorting the respective influence of grain-boundary friction versus bulk structural changes. Along this line, we started with a simple situation of low friction steel beads with frictional boundaries but of a roughness much smaller than a grain size. A second situation is studied where the granular material is made of rugous polydisperse glass beads.

II. EXPERIMENTAL SETUP

Most experiments are performed on dry, noncohesive, and monodisperse steel beads of diameter $d=1.58$ mm piled into a vertical duralumin or brass cylinder of diameter $D=36$ mm. We also perform a series of experiments on a miscellany of glass beads of three diameters (1.5 mm, 2 mm, and 3 mm) with equal volume of each kind, in a poly(methyl methacrylate) (PMMA) cylinder. The column is closed at the bottom by a movable brass piston avoiding contact with the column (diameter mismatch is 0.5 mm). A force probe of stiffness $k=40\,000$ N m^{-1} is located under the piston and is pushed at a constant driving velocity V (between 5 nm s^{-1} and 100 μm s^{-1}) via a stepping motor (see Fig. 1). The resistance force F encountered by the piston is measured as a function of time. We also monitor the relative humidity (χ) and the surrounding temperature. We work in the range $35\%<\chi<75\%$, as well as in dry air ($\chi<3\%$) and humid air ($\chi=90\%$). Actually, except for the dry and humid situations, we do not regulate this last parameter (χ) but we record its values close to the experimental setup. We obtain dry air by having a weak air flux (250 ml min^{-1}) flow into a cylinder filled with silica. We obtain humid air by making a weak air flux (250 ml min^{-1}) bubble through water. Then, for the duration of an experiment, weak fluxes of humid or dry air are set to flow through the column from top to bottom, maintaining a constant and homogeneous level of humidity. Note that a stationary relative humidity is reached in a few minutes. We start our experiments when this stationary level is attained. We verified that the weak air flux does not perturb the system: we notice no evolution of the force when the flux is stopped as long as relative humidity remains unchanged. Temperature is kept at $(20\pm1)\,^{\circ}$C. We actually find no correlation between the force fluctuations and the temperature variations in this range.

Note that the brass and duralumin cylinders have very different surface properties (Fig. 2). The duralumin cylinder is rough cast, and its roughness is 400 nm. The brass cylinder was machine turned, and has a mean roughness of 7 μm with undulations of wavelength 100 μm and depth 25 μm. Note that this roughness is much smaller than a grain size

In order to compare precisely the rheological properties of granular assemblies to solid friction properties, we built a special device (called ''the slider,'' see Fig. 1 inset) designed to study the tribology of bead-wall contact. This device is set to apply a constant normal load ($F_N=2$ N) on three steel beads sliding vertically on the cylinder's wall. Then, the dynamical evolution of the resistance force encountered by the piston pushing a granular material can be compared to the slider's friction resistance driven in the same conditions.

Two granular systems will be studied. First, a model assembly of monodisperse steel spheres and second a polydisperse assembly of rough glass beads. The largest part of this paper is devoted to the monodisperse assembly.

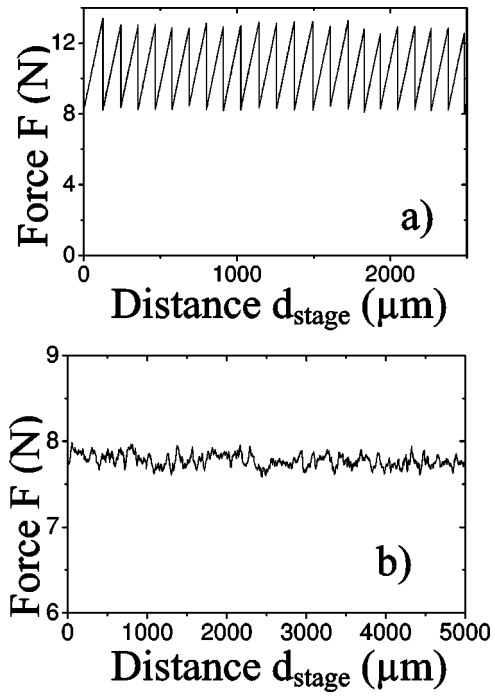

FIG. 3. Resistance force to pushing of a height $H=2.15D$ (380 g) of steel beads in the duralumin cylinder vs displacement d_{stage} of the translation stage; (a) in the stick-slip regime ($V=30$ nm s^{-1}), (b) in the steady-sliding regime ($V=100$ μm s^{-1}).

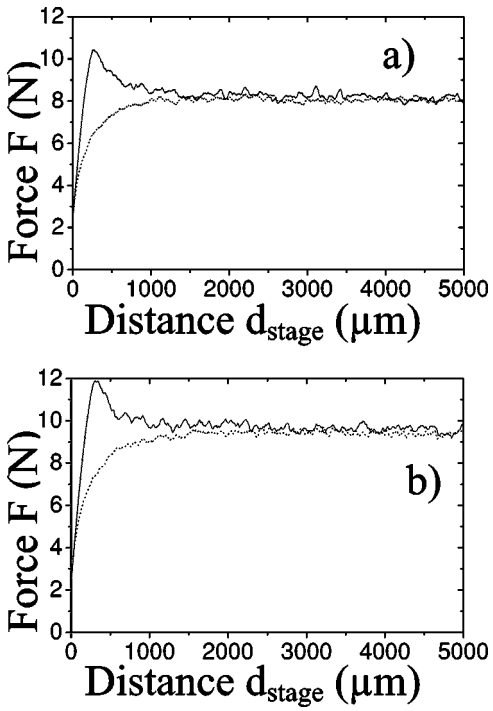

FIG. 4. Evolution of the resistance force in the steady-sliding regime for two different initial packings: a dense one (65%) and a loose one (59%); the full line is for the initially dense packing, the dotted line is for the initially loose packing. (a) $V=20$ μm s^{-1}; (b) $V=100$ μm s^{-1}.

III. MONODISPERSE STEEL BEADS

We now report on the simplest situation, i.e., monodisperse low frictional steel beads in a duralumin or brass cylinder. We observe two distinct dynamical stationary regimes (Fig. 3): for high driving velocities, the motion is characterized by a steady sliding and a constant pushing force; for low velocities, the system undergoes a dynamic instability characterized by a stick-slip motion.

We first note that as far as averaged packing fraction and pushing force are concerned, whatever the initial state of preparation is, the same stationary regime is reached (Fig. 4). When a dense packing ($\overline{\nu}=65.0\pm0.5\%$) is prepared by rain filling, the force in the steady-sliding regime increases up to a maximum, then decreases slowly for a piston displacement of about 3 mm. At this point where a stationary value $\overline{F}$ of the force is attained, the average packing fraction $\overline{\nu}$ is $62.5\pm0.5\%$. In the case of an initially loose packing ($\overline{\nu}=59.0\pm0.5\%$), prepared by using an inner cylinder slowly removed after filling, the force in the steady-sliding regime increases monotonically for a 3-mm displacement before the same stationary value $\overline{F}$ of force is reached. This state is also characterized by a 62.5% packing fraction. For all preparations, we always get a stationary regime characterized by the same pushing force $\overline{F}$, which depends on driving velocity V, relative humidity χ, and packing's height H, as well as the same packing fraction ($\overline{\nu}=62.5\pm0.5\%$), independent of V, χ, and H. The stick-slip regime displays a similar phenomenology: the piling reaches a stationary packing fraction of $\overline{\nu}=62.5\pm0.5\%$; in the transitory regime, the pushing force for dense packing displays a maximum and for a loose packing shows a monotonous increase. In Sec. III A 1, we propose an explanation for the phenomenology of the transitory regimes.

We are aware that there is always ordering at the wall for monodisperse packing of hard spheres, and shearing such a granular material can induce crystallization effects [22]. We cannot prevent this ordering since, at steady state, general packing properties and the granular rheology impose it. Nevertheless, for a flat interface (after pouring), ordering at a boundary is never larger than 3–4 grain sizes (see, for example Ref. [23]). Moreover, here, we have a curved boundary that prevents further the extension of a crystalline ordering in the bulk. To be more precise, an experiment was performed by Vanel [24], in the same geometrical conditions: the packing was invaded by a polymeric resin, then solidified and sliced. The organization effect at the wall was clear but did not go over 2 grain sizes. Furthermore, we measure a packing fraction of 0.625 ± 0.005 constant in time. This is an average quantity close enough to the random close packing limit. Thus, it means for us that in the following, the global redirection properties captured by Janssen's coefficient K are bulk effects essentially due to a randomly packed material (but not necessarily isotropic).

In the following, we present the phenomenology observed in the steady-sliding and the stick-slip regime, when the stationary state is attained. For each regime, we first focus on the mechanical properties and propose a model accounting for friction at the walls and bulk properties; we then study and analyze the rheological properties. In Sec. III C, we point

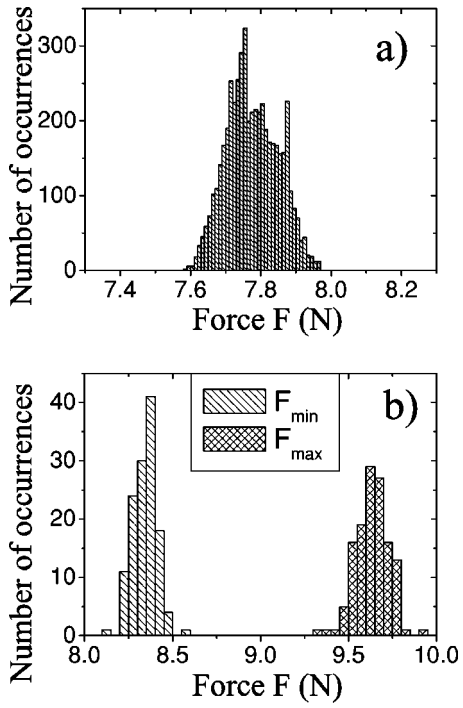

FIG. 5. (a) Distribution of the resistance force value for every micrometer during 5 mm of sliding in the steady-sliding regime of Fig. 3(b) at $V=100\ \mu\mathrm{m\,s^{-1}}$. (b) Distribution of the maximum and minimum resistance forces F_{max} and F_{min} in the stick-slip regime of Fig. 3(a) at $V=30\ \mathrm{nm\,s^{-1}}$ during 5 mm of sliding.

out ambiguity of dependence on relative humidity. We then analyze our results in a standard solid-on-solid friction framework (the Dieterich-Ruina model). Finally, we study the transition from steady-sliding to stick-slip regime.

A. Steady sliding

For a given height of beads in the column, at given driving velocity V and relative humidity χ, the force in the steady-sliding regime is constant within 2% [Fig. 5(a)], and its distribution around mean value $\overline{F}$ is nearly Gaussian.

Next, we study the behavior of mean pushing force $\overline{F}$ as a function of the packing height, the driving velocity, and the relative humidity.

1. Mechanical properties

For a vertically pushed granular assembly, the driving force exerted by the piston is screened due to friction with the walls. To evaluate this effect, the mean resistance force $\overline{F}$ in the steady-sliding regime is measured as a function of the packing height (see Fig. 6).

The resistance force $\overline{F}$ increases very rapidly with packing's height H. Following the standard Janssen screening picture, this strong resistance to motion is due to the leaning of the granular material on the walls created by the horizontal redirection of vertical stress in association with solid friction at the sidewalls. It means that we may relate horizontal and vertical stresses averaged on a slice at height z by an effective relation

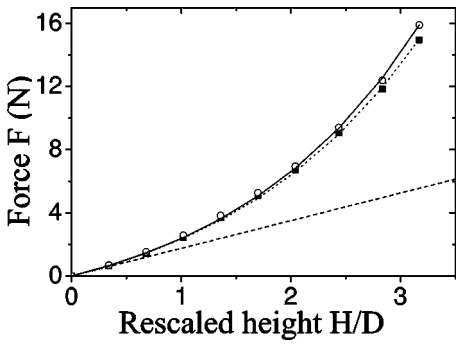

FIG. 6. Mean resistance force in the steady-sliding regime as a function of the height H of the packing scaled by the column diameter D, for steel beads in the duralumin column, for $V=16\ \mu\mathrm{m\,s^{-1}}$ (filled squares) and $V=100\ \mu\mathrm{m\,s^{-1}}$ (open circles). The solid line and the dotted line are fits by Eq. (3). The dashed line is the hydrostatic curve.

$$\sigma_{zz}(z)=K\sigma_{rr}(z), \tag{1}$$

where K is called Janssen's redirection constant. At the walls, we suppose a sliding of the granular material at a velocity V_0 (the driving velocity); the shearing stress is then

$$\sigma_{rz}(z)=\epsilon\mu_d(V_0)\sigma_{rr}(z), \tag{2}$$

where $\mu_d(V_0)$ is the dynamic coefficient of friction between the beads and the cylinder's wall at a velocity V_0. The constant $\epsilon=\pm 1$ is introduced in order to differentiate between pushing and pulling experiments. When $\epsilon=+1$, the granular material is moving upwards and friction is fully mobilized downwards (our pushing experiment); and when $\epsilon=-1$, the granular material is moving downwards and friction is fully mobilized upwards.

The force $\overline{F}_\varepsilon$ exerted by the grains on the piston can be derived from equilibrium equations for all slices, thus we obtain

$$\overline{F}_\epsilon=\varrho g\lambda\pi R^2\epsilon\left[\exp\left(\epsilon\frac{H}{\lambda}\right)-1\right], \tag{3}$$

where ϱ is the mass density of the granular material, R is the cylinder radius, and g is gravity acceleration. The length $\lambda=R/2K\mu_d(V_0)$ is the effective screening length.

It is easily seen from Eq. (3) that when $\epsilon=+1$, any slight change in μ or K is exponentially amplified with a drastic influence on the pushing force $\overline{F}$. In the steady state-regime, the experimental data obtained for a given pushing velocity V can be fitted by relation (3) by adjusting only one parameter, i.e.,

$$p_{+1}=K\mu_d(V_0), \tag{4}$$

where $\mu_d(V_0)$ is the dynamic coefficient of friction at velocity V_0.

We see in Fig. 6 that the data are well fitted by Eq. (3) and, for a relative humidity $\chi=45\%$, for steel beads in the duralumin cylinder, we obtain $p_{+1}=0.140\pm0.001$ at $V_{up}=16\ \mu\mathrm{m\,s^{-1}}$ and $p_{+1}=0.146\pm0.001$ at $V_{up}=100\ \mu\mathrm{m\,s^{-1}}$.

We are now able to propose an interpretation of the features observed for different initial packing fractions within Janssen's framework. Since Janssen's coefficient K is an increasing function of the packing fraction, as it was shown previously [25,19], the resistance force of an initially dense packing displays a maximum, as a dense packing leans more efficiently on walls than a loose one; the pushing force then decreases while the packing loosens (i.e., while K decreases). On the other hand, for an initially loose packing the resisting force in the transitory regime will increase while the packing densifies (i.e., while K increases).

For an initially dense packing, we extract a parameter p_{+1}^{max} from a fit of the pushing force maximum value in the transitory regime with formula (3): we obtain $p_{+1}^{max} \approx 0.18$ at $V_{up} = 16\ \mu\mathrm{m\,s}^{-1}$ and $p_{+1}^{max} \approx 0.18$ at $V_{up} = 100\ \mu\mathrm{m\,s}^{-1}$; as this experiment was not repeated sufficiently, we do not have uncertainties on these values. Nevertheless, we note that the p_{+1}^{max} value is roughly 25% higher than the p_{+1} stationary value, whatever the velocity is. These results are consistent with a K dependence on compacity $\overline{\nu}$ derived in Ref. [19] for an assembly of monodisperse glass beads, i.e., $\Delta K/K \approx 5\Delta\overline{\nu}/\overline{\nu}$; for initial compacity 65% and steady-state compacity 62.5%, this empirical formula actually leads to $\Delta K/K \approx 0.2$. Therefore, in Janssen's framework, we are led to attribute the difference between maximum force and stationary force to a difference in stress redirection (i.e., in K) due to a difference in compacity. The force history in the transitory regime would then just reflect the compacity history.

As a check of consistency, we perform the following dynamical experiment. First, the granular column is pushed upwards in order to mobilize the friction forces downwards and far enough to reach the steady-state compacity. Starting from this situation, the friction forces at the walls are reversed by moving the piston downwards at a constant velocity $V_{down} = 16\ \mu\mathrm{m\,s}^{-1}$, until a stationary regime is attained. Note that this stationary regime is characterized by the same compacity $\overline{\nu} \approx 62.5\%$ as in the pushing situation. Following relation (3), this procedure would imply a change of ϵ from 1 to -1 and consequently, the dynamical force on the piston should decrease from $\overline{F}_{+1}$ to $\overline{F}_{-1}$. In Fig. 7, the pushing force $\overline{F}_{-1}$ is measured for different packing heights H. The fit of experimental results with Eq. (3) gives $p_{-1}(16\ \mu\mathrm{m\,s}^{-1}) = 0.156 \pm 0.002$, which is 10% larger than $p_{+1}(16\ \mu\mathrm{m\,s}^{-1})$. This difference, though small, can be observed out of uncertainties, and is systematic. It cannot be due to a slight change in compacity $\overline{\nu}$ as from relation $\Delta K/K \approx 5\Delta\overline{\nu}/\overline{\nu}$, we would expect a 2% variation in compacity between the pushing and the pulling experiments, which would be observed; we actually measured $\Delta\overline{\nu}/\overline{\nu} = 0 \pm 1\%$. According to Janssen's picture, this would imply that vertical stress redirection is more efficient in the downward pulling situation. We believe this is a clear evidence of a granular structuration effect but it also shows that this effect is not dominant: it affects only 10% of the average mechanical parameter K.

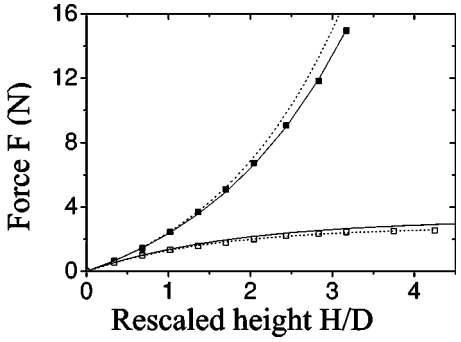

FIG. 7. Resistance force to pushing (filled squares) and to pulling (open squares) in the steady-sliding regime at $V = 16\ \mu\mathrm{m\,s}^{-1}$ as a function of the height H of the packing scaled by the column diameter D, for steel beads in the duralumin column. The solid lines are the fit with Eq. (3) of the resistance force to pushing and its prediction for the pulling situation; the dotted lines are the fit with Eq. (3) of the resistance force to pulling and its prediction for the pushing situation.

We have shown in another report that in a Janssen experiment, an isotropic homogeneous elastic material can also be characterized by stress redirection properties [19]. For a granular column at high depth, an effective relation

$$\sigma_{zz} = K_{el}\sigma_{rr} \tag{5}$$

is obtained with

$$K_{el} = \nu_p/(1-\nu_p), \tag{6}$$

where ν_p is the material's Poisson coefficient. This actually leads to a curve similar to Janssen's saturation curve as long as friction at the walls is small (typically less than 0.5). In order to get the isotropic homogeneous elasticity prediction for the pushing experiment, we perform a series of numerical simulations using finite element method [26]. The column is modeled as an isotropic elastic medium. We vary the friction μ_d at the walls, the Young modulus E, and the Poisson coefficient ν_p. We impose a rigid, either perfectly stick or perfectly slip bottom. We find no appreciable difference between these two previous cases. The condition $\sigma_{rz} = -\mu_d\sigma_{rr}$ is imposed everywhere at the walls (for the pulling situation, we impose $\sigma_{rz} = +\mu_d\sigma_{rr}$). The cylinder is modeled as a duralumin elastic medium. As long as the Young modulus E of the elastic medium is less than 500 MPa, which is usually the case for granular media, we find no dependence of the results on E. We verified that in all the simulations we performed, there is no traction in the elastic medium, so that this could be a fair modeling for a granular material.

We find no appreciable difference between the elastic prediction (Fig. 8) and the curve given by Eq. (3) with $K = K_{el}$. Therefore, regarding the dependence of the stationary state force $\overline{F}$ on the height of beads, our system cannot be distinguished from an elastic medium.

Note that finite element simulations show that the presence of a rigid bottom implies that the effective Janssen's parameter K_{eff} extracted from Janssen's scaling for the pull-

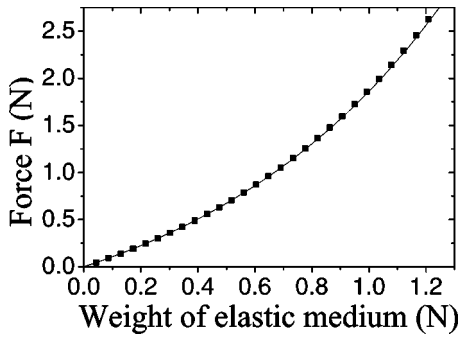

FIG. 8. Comparison of the resistance force to pushing simulated for a homogeneous isotropic elastic medium (squares) of Poisson coefficient $\nu_p = 0.45$ and Young modulus $E = 100$ MPa in a duralumin cylinder, with coefficient of friction $\mu = 0.2$ at the walls, to the curve obtained with Eq. (3) with Janssen coefficient $K = K_{el} = \nu_p/(1-\nu_p) = 0.82$ (full line).

ing situation is higher than K_{el} [19], whereas for the pushing $K_{eff} \approx K_{el}$ (as can be seen in Fig. 8: the fit of the elastic curve with $K = K_{el}$ is good). Details on this numerical work will be given elsewhere [20]. Actually, if we adjust the elastic predictions for pushing and pulling experiments with an elastic material of Poisson coefficient $\nu_p = 0.45$, Eq. (3) yields a Janssen's constant K_{eff} for the pushing which is about 3% lower than K_{eff} for the pulling. This is qualitatively (though not quantitatively) in agreement with the experimental results. Then isotropic elasticity can be a good framework only if we neglect the existence of bulk structuration effects inducing differences in the effective Poisson coefficient of the material between the pulling and the pushing. Note that in this case, an isotropic modeling of the granular material is somehow questionable.

In a previous study [25], it was found that Janssen's picture has a general tendency to slightly underestimate the stress below a granular column for a homogeneous packing of glass beads. We have showed in another report that it is no more true as the friction at walls is very well controlled. Therefore, this model, though elementary, seems a fair base for analysis and provides an analytical expression from which constitutive rheological parameters can be extracted. A central question is still that the fitting parameters $p = K\mu_d$, extracted from the model, do not allow to distinguish between μ_d and K separately.

In the following, we will show experiments which aim at sorting out the relative contributions of wall-bead interactions (i.e., μ_d) and bulk properties (i.e., K), which have an influence on the rheological properties when velocity and relative humidity are changed.

2. Rheological properties

The mean resistance force $\overline{F}$ in the steady-sliding regime increases strongly when the velocity and the relative humidity are increased. In the duralumin column (Fig. 9), the resistance force $\overline{F}$ at velocity $V = 100\ \mu\mathrm{m\,s^{-1}}$ is 60% higher for relative humidity $\chi = 73\%$ than for $\chi = 40\%$; near the transition to the stick-slip regime ($V = 1\ \mu\mathrm{m\,s^{-1}}$), dependence of $\overline{F}$ on χ is much less important, and there is actually

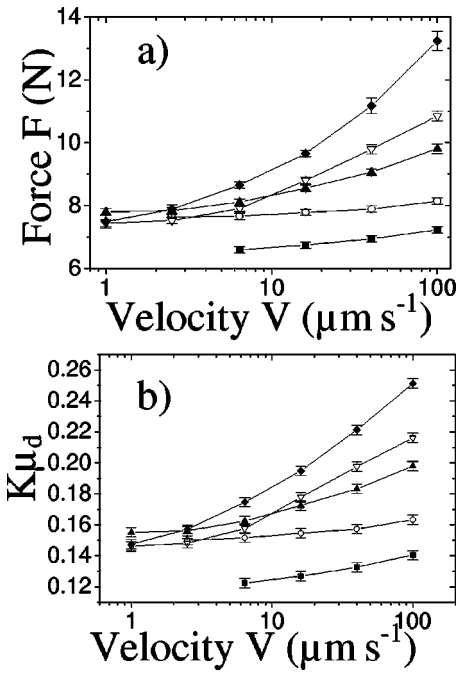

FIG. 9. (a) Mean force $\overline{F}$ in the steady-sliding regime for height $H = 2.15D$ (380 g) of steel beads in the duralumin cylinder, for various relative humidities χ: 72% (diamonds), 66% (open inverted triangles), 53% (triangles), 40% (open circles), and $<3\%$ (squares). (b) Coefficient $K\mu_d$ extracted from a fit of $\overline{F}$ with formula (3).

no difference in $\overline{F}$ values for χ varying between 40% and 73%. Another important feature is that the increase of $\overline{F}$ with velocity is sharper when χ is higher. In the brass column (Fig. 10), the mean resistance force $\overline{F}$ also increases with relative humidity χ, but now the variation coefficient with velocity (the slope in Fig. 10) does not seem to depend on χ. Moreover, for a velocity $V = 100\ \mu\mathrm{m\,s^{-1}}$, increase of $\overline{F}$ is only 15% from dry to humid ($\chi = 90\%$) atmosphere.

The fit of $\overline{F}$ with Janssen's formula adapted to the pushing case of Eq. (3) gives parameter $K\mu_d(V)$ for different relative humidities χ. The fundamental differences of behavior in the steady-sliding regime between the duralumin column and the brass column for a same granular material, at same density, suggest that the variations in χ and velocity have an influence mainly on the coefficient of friction μ_d at the walls and little on the mechanical properties of the granular material (i.e., K). Therefore, in the following analysis, we will consider K as a constant at first order of approximation.

Steel/duralumin. Figure 9 shows that dynamical parameter $K\mu_d$ is globally less important in a dry atmosphere than in the ambient atmosphere. In ambient atmosphere ($40\% < \chi < 73\%$), a change in χ seems to change only the variation coefficient of $K\mu_d$ with velocity, i.e., the increase of $K\mu_d$ with velocity is sharper when χ is higher. This phenomenon could be interpreted as a viscous contribution of the water condensed at the contacts. Note that this phenomenology contrasts with the observations of Riedo *et al.* [5], who found, for solid-on-solid nanoscopic sliding friction mea-

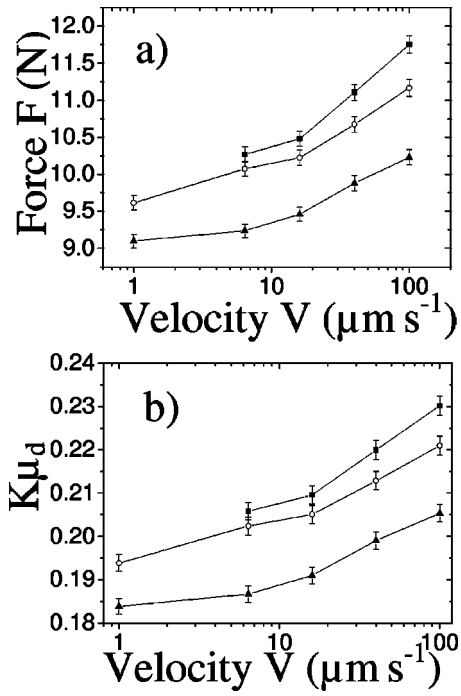

FIG. 10. (a) Mean force $\overline{F}$ in the steady-sliding regime for height $H=2.15D$ (380 g) of steel beads in the brass cylinder, for various relative humidities χ: 90% (squares), 53% (open circles), and $<3\%$ (triangles). (b) Coefficient $K\mu_d$ extracted from a fit of $\overline{F}$ with formula (3).

surements, that in all the systems they studied, of various wettability, the effect of a humidity increase is to add a negative value to the coefficient of friction force dependence on logarithm of velocity. Table I shows the results of a rough logarithmic fit of data with $\mu_d(V)=\mu_0+(a-b)\ln(V/V_0)$. We use the parameter $(a-b)$ as a standard reference to the Dieterich-Ruina model [27,28].

We observe that the increase rate $K(a-b)$ of $K\mu_d$ with the logarithm of velocity is multiplied by 7 when χ increases from 40% to 72%.

In order to compare these results with those obtained in a solid-on-solid friction experiment, we need to evaluate Janssen's parameter K. We extract K from a classical Janssen experiment [19] and we obtain $K\mu_s=0.184\pm0.002$ for a mean aging time of 40 seconds. From the measurement of static friction, using the sliding angle of a three bead tripod, we extract $K=1.02\pm0.07$.

TABLE I. Parameter $K(a-b)$ extracted from a fit of $K\mu_d$ with formula $\mu_d(V)=\mu_0+(a-b)\ln(V/V_0)$ for different relative humidities χ in the duralumin column.

Relative humidity χ (%)	$K(a-b)$
<3	0.0065 ± 0.0006
40	0.004 ± 0.0005
53	0.013 ± 0.001
66	0.021 ± 0.0005
72	0.028 ± 0.0015

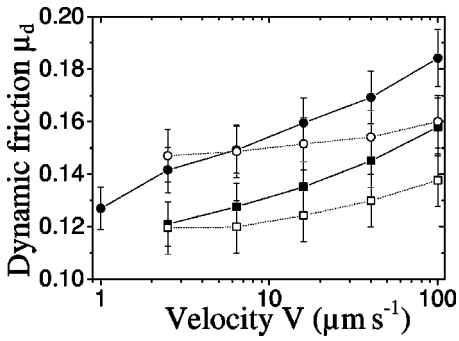

FIG. 11. Dynamical coefficient of friction μ_d extracted from a fit of $\overline{F}$ with Janssen's formula adapted to pushing (open symbols) for a height $H=2.15D$ (380 g) of steel beads in the duralumin cylinder, and μ_d measured in a solid-on-solid experiment (filled symbols), for two relative humidities χ: 40% (circles) and $<3\%$ (squares).

We suppose K is constant and is not affected by any variation in relative humidity or velocity. The dynamical coefficient of friction obtained in a solid-on-solid friction experiment with the slider (Fig. 1 inset) is then compared, in Fig. 11, with the one extracted from a fit of the resistance force with formula (3). Note that the uncertainty on μ_d extracted from formula (3) is mainly systematic (coming from uncertainties on K, which themselves come from uncertainty on static friction measurements). We observe that the dynamical coefficients of friction measured in a solid-on-solid experiment increase slightly more strongly with velocity than the one extracted from the resistance force of the granular material. But importantly, the increase of μ_d with relative humidity χ is the same in both cases.

In this analysis, we assumed a constant value for Janssen's coefficient K. We can also imagine a slight decrease of K with increasing velocity so that the solid-on-solid μ_d would match the one extracted from the pushing experiment. However, we will remain prudent as the mean pressure contact on beads in the solid on solid experiment is much higher than in the granular column, which may cause quantitative differences between friction properties. More precisely, at the bottom of the column, for a pushing force $\overline{F}=10$ N, the mean contact force per bead is about 20 mN; a Hertz contact would give mean contact pressure $\overline{p}\simeq300$ MPa. For a contact force per bead of 2 N (the slider case), a Hertz contact would give $\overline{p}\simeq1300$ MPa.

Steel/brass. In the brass column, we observe the same phenomenology as in the duralumin one, i.e., an increase of $K\mu_d$ with velocity and relative humidity χ. The effect of a change in χ is yet less important than in the duralumin column, as the coefficient $K\mu_d$ increases only by 15% at velocity $V=100$ μm s^{-1} when χ increases from 0% to 90%. A major difference with the duralumin column is that in the brass column, a variation in χ seems to induce a variation of friction but hardly affects the coefficient of variation with velocity (the slope). Table II shows the results of a logarithmic fit of the data with the function: $\mu_d(V)=\mu_0+(a-b)\ln(V/V_0)$. We observe indeed that the slope $K(a-b)$ of $K\mu_d$ with the logarithm of velocity does not practically vary

TABLE II. Parameter $K(a-b)$ extracted from a fit of $K\mu_d$ with formula $\mu_d(V)=\mu_0+(a-b)\ln(V/V_0)$ for different relative humidities χ in the brass column.

Relative humidity χ (%)	$K(a-b)$
<3	0.007 ± 0.001
53	0.007 ± 0.001
90	0.0085 ± 0.0015

with relative humidity χ, and is much weaker than in the duralumin column.

The comparison with the slider and the differences between the duralumin and brass columns suggest that the rheological properties in the steady-sliding regime are dominated by the friction properties at the walls. We now investigate the stick-slip regime.

B. Stick-slip regime

In the stick-slip regime, for a given height of beads in the column and at given driving velocity V and relative humidity χ, the maximum force before a slip and the minimum force at the end of a slip are constant within 2% [Fig. 5(b)]. Their distribution around mean values F_{max} and F_{min} is nearly Gaussian.

The dynamical evolution $F(t)$ of the pushing force during the slip phase can be translated into a function of the granular material instantaneous velocity. Motion of the granular material at velocity V induces a variation $dF=k(V_0-V)dt$ of resistance force during time dt, where k is the force probe stiffness and V_0 the driving velocity; we thus obtain $V(t)=V_0-dF/kdt$. We see (Fig. 12) that the acceleration and deceleration phases are nearly symmetric. This phenomenology is currently observed in solid friction experiments. This is in contrast with previous plane shearing experiments of granular materials [9] in which the deceleration phase would occur in two steps, first fast and then slow. However, a major difference is that in the latter case, the displacements during slippage are millimetric (a grain size) whereas in our experiment, they are micrometric (30 μm in Fig. 12). As a consequence, the evolution of forces observed during a slip seems to reflect the slippage of grain contacts at the walls. The maximum velocities obtained during the slip phase are of a few hundred $\mu\mathrm{m\,s^{-1}}$. We did not study systematically the variation of instantaneous velocity with bead height or with driving velocity.

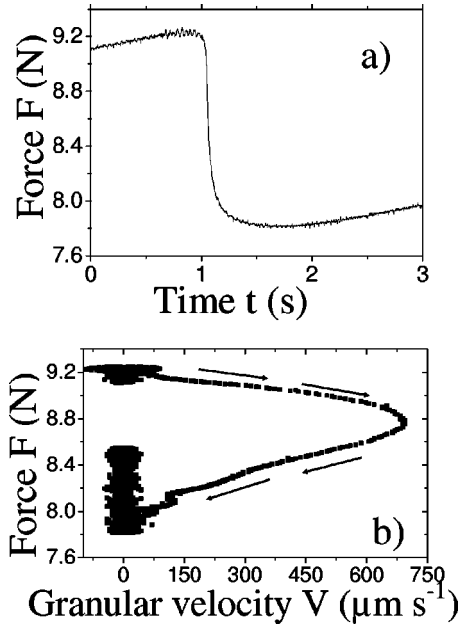

FIG. 12. (a) Force vs time for a slip event in the stick-slip regime at $V=1$ $\mu\mathrm{m\,s^{-1}}$ for a height $H=2.15D$ (380 g) of steel beads in the duralumin column. (b) Force vs velocity of the granular material for the slip event of (a).

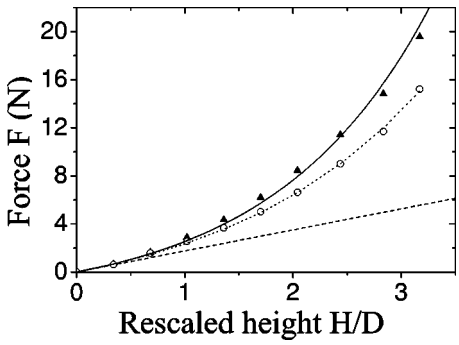

FIG. 13. Mean maximum and minimum resistance forces F_{max} (filled triangles) and F_{min} (open circles) in the stick-slip regime as a function of the height H of the packing scaled by the column diameter D, for steel beads in the duralumin column, for stick time $t_{stick}=40$ s. The solid and dotted lines are fits by Eq. (8). The dashed line is the hydrostatic curve.

In the following, we report on the F_{max} and F_{min} properties as a function of the packing height, the driving velocity, and the relative humidity.

1. Mechanical properties

In the stick-slip domain, the mean maximum and minimum resistance forces F_{max} and F_{min} are measured as functions of the packing height (see Fig. 13), but now we choose to perform our experiments not at a constant velocity V but at constant stick time t_{stick}, and we explain why in the following.

Experimentally, we find that the resistance forces F_{max} and F_{min} increase exponentially with packing's height H. The data can actually be fitted by a formula such as Eq. (3), but the parameter p_{+1} extracted may be different and should not depend on $\mu_d(V_0)$ as the granular material is not sliding during stick, and does not slide at driving velocity V_0 during slip.

The model can actually be simply modified for this situation. In the stick-slip regime, when the resistance force $F(t)$ is equal to F_{max}, the material just starts slipping, which means that static friction is fully mobilized at this instant for each contact. So we can write $\sigma_{rz}=\mu_s\sigma_{rr}$ everywhere at the walls, where μ_s is static friction between beads and the cylinder's walls. Static friction coefficients are known to evolve in time [29], we then have to include aging effects. As the

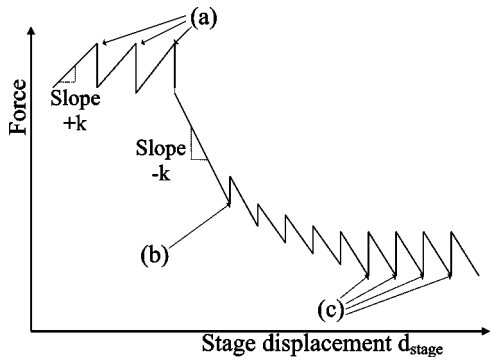

FIG. 14. Sketch of the method for measuring forces at the onset of slipping in the pushing and pulling situations. (a) refers to the maximum force before a slip in the stationary stick-slip regime in the pushing experiment; (b) refers to the minimum force before the first slip in the pulling experiment after the material has been pushed over 5 mm; (c) refers to the minimum force before a slip in the stationary stick-slip regime in the pulling experiment.

granular material was at rest in the column since the previous slip, aging time in this situation is the time of stick

$$t_{stick}=\frac{F_{max}-F_{min}}{kV_0}. \tag{7}$$

So the final formula for F_{max} in Janssen's framework is

$$F^{\epsilon}=\varrho g\lambda\pi R^2\epsilon\left[\exp\left(\epsilon\frac{H}{\lambda}\right)-1\right], \tag{8}$$

where the screening length is now $\lambda=R/2K\mu_s(t_{stick})$. Here again, $\epsilon=+1$ for a pushing experiment (i.e., $F_{max}=F^{+1}$), $\epsilon=-1$ for a Janssen experiment. The choice of imposing a constant stick time t_{stick} instead of a constant driving velocity V_0 for the experiments in the stick-slip regime is now justified by the dependence of μ_s on t_{stick}, whereas μ_d depends on V_0.

In the steady-state regime, the experimental data obtained for a given stick time t_{stick} can be fitted by relation (8) by adjusting only one parameter, i.e., $p_{+1}=K\mu_s(t_{stick})$, where $\mu_s(t_{stick})$ is the static coefficient of friction for an aging time t_{stick}. For the data of Fig. 13 obtained for a relative humidity $\chi=40\%$ with a mean stick time of 40 s, we find $p_{+1}=0.184\pm0.002$ from F_{max} [F^{+1} in Eq. (8)]. Note that, though friction is not fully mobilized when $F=F_{min}$, the fit of F_{min} with Eq. (8) is good (Fig. 13); we obtain a parameter $p_{+1}=0.148\pm0.002$ which should not be related to $\mu_s(t_{stick})$ in that case.

As a check of consistency, we perform the following dynamical experiment in the stick-slip regime. First, the granular column is pushed upwards in order to mobilize the friction forces downwards and to reach the steady-state compacity; F_{max} (referred to as *a* in Fig. 14) is then measured for constant stick time t_{stick}. Starting from this situation, the friction forces are reversed at the walls by moving the piston downwards. We then measure the force F_{min} of the first slip (referred to as *b* in Fig. 14) after the same time t_{stick}. Please, be aware that the roles of F_{min} and F_{max} are inverted in the pulling experiment: F_{min} is the minimum force before a slip and F_{max} is the maximum force at the end of a slip. We also measure mean minimum force F_{min} (referred to as *c* in Fig. 14) when a steady stick-slip regime is reached in the pulling experiment. Note that this stationary regime is characterized by the same compacity $\overline{\nu}\approx62.5\%$ as in the pushing situation.

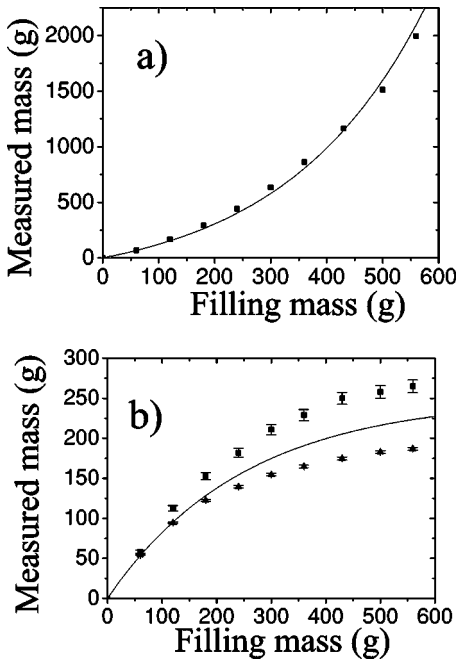

FIG. 15. (a) Mean maximum resistance force measured in the stick-slip regime as a function of the height *H* of the packing scaled by the column diameter *D*, for steel beads in the duralumin column, for stick time $t_{stick}=40$ s; the line is a fit with Eq. (8). (b) Measured mass vs filling mass for a classical Janssen experiment obtained in two different ways: we plot the mass of the first slipping event (squares), and the mean minimum mass in the stationary stick slip for the pulling situation (triangles); the line is the Janssen curve predicted with the parameter extracted from the pushing experiment of (a).

Following relation (8), this procedure should imply a change of ϵ from 1 to -1 and, consequently, the force at the onset of slipping on the piston should decrease from F^{+1} to F^{-1}. As we observed no noticeable variation of compacity between the pushing and the pulling, we expect Janssen's parameter *K* value to be unchanged. In Fig. 15, the pulling force F^{-1} is measured for different packing heights *H*, for the first slipping event, and in the steady stick-slip regime. The fit of experimental results with Eq. (8) gives $p_{-1}(40\text{ s})=0.230\pm0.004$ for stationary stick slip, which is 20% larger than $p_{+1}(40\text{ s})$. It cannot be due to a slight change in average compacity $\overline{\nu}$ as from relation $\Delta K/K\approx5\Delta\overline{\nu}/\overline{\nu}$, we would expect a 4% variation in compacity, which would have been observed; let us recall that we actually measured a compacity variation between the pushing and the pulling experiments $\Delta\overline{\nu}/\overline{\nu}=0\pm1\%$.

As in the steady-sliding experiment, according to Janssen's picture, this would then imply that vertical stress redi-

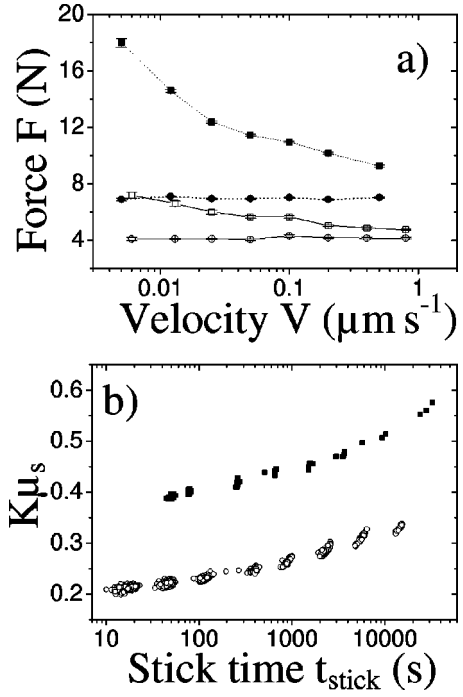

FIG. 16. (a) Minimum and maximum resistance forces F_{min} (circles) and F_{max} (squares) vs driving velocity in the stick-slip regime for a height $H=1.4D$ (250 g) of steel beads in the duralumin cylinder, for relative humidities $\chi=90\%$ (filled symbols) and $\chi=45\%$ (open symbols). (b) $K\mu_s$ as a function of stick time t_{stick} for a height $H=1.4D$ (250 g) of steel beads in the duralumin cylinder, for relative humidities $\chi=90\%$ (filled squares) and $\chi=45\%$ (open circles).

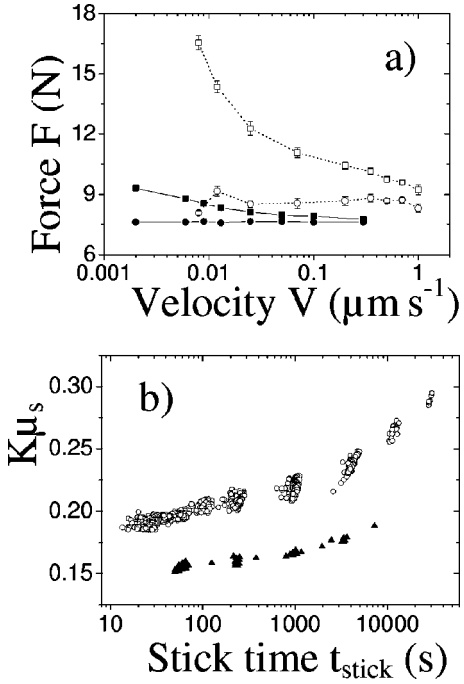

FIG. 17. (a) Minimum and maximum resistance forces F_{min} (circles) and F_{max} (squares) vs driving velocity in the stick-slip regime for a height $H=2.15D$ (380 g) of steel beads in the duralumin cylinder, for relative humidities $\chi=45\%$ (open symbols) and $\chi<3\%$ (filled symbols). (b) $K\mu_s$ as a function of stick time t_{stick} for a height $H=2.15D$ (380 g) of steel beads in the duralumin cylinder, for relative humidities $\chi=45\%$ (open circles) and $\chi<3\%$ (filled triangles).

rection is more efficient in the pulling situation; furthermore, this effect is enhanced in the stick-slip regime. For the first slip event in the pulling experiment, we find $p_{-1}(40\ \mathrm{s})=0.16\pm0.015$, which is now lower than $p_{+1}(40\ \mathrm{s})$. We believe that this is a clear evidence of granular structuration effects. We interpret the differences in p_{-1} values by saying that the packing has first been structured to resist the pushing. When we start pulling, structure is not efficient to resist the pulling, and it results in a lower Janssen's constant (therefore lower p_{-1}) for the first slip event; when we continue pulling, the packing gets structured to resist pulling and leans more efficiently on the walls, i.e., Janssen's constant (and p_{-1}) increases. Moreover, steady-state structuration is more efficient for the pulling than for the pushing, which means that both structurations may be different and could reflect the symmetry breaking due to gravity.

The results of the simulations of an elastic medium in a column presented in the precedent section for a steady sliding also carry on to the stick-slip situation. If we impose numerically everywhere at the walls, the relations $\sigma_{rz}=\boldsymbol{\mu_s}\sigma_{rr}$ or $\sigma_{rz}=\boldsymbol{\mu_d}\sigma_{rr}$, it would merely correspond to a change in the name of the friction coefficient. The equilibrium equations are the same for the static and steady dynamic cases. The important common point is that friction forces are fully mobilized everywhere at the walls. Therefore, as for the steady sliding, the data can be fitted by the elastic predictions, and the 3% difference in Janssen's parameter between the pulling and the pushing of an elastic medium of constant Poisson ratio is again qualitatively (though not quantitatively) in agreement with the experimental results.

In the following, as we study the steady-state regime, we will try to distinguish between wall-bead interactions (i.e., μ_s) and the bulk properties (i.e., K) as they influence the rheological properties when velocity and relative humidity are changed.

2. Rheological properties

The mean maximum force F_{max} increases strongly when the driving velocity V_0 is decreased and the relative humidity χ is increased [Figs. 16(a), 17(a), and 18(a)]. Furthermore, apparent divergence of F_{max} when V_0 decreases is enhanced when χ increases. The mean minimum force F_{min} is almost independent of the driving velocity, and increases when the relative humidity is increased [Figs. 16(a), 17(a), 18(a)]. For each stick-slip event, an aging time (the stick time) is measured: $t_{stick}=(F_{max}-F_{min})/(kV)$. This time is associated to a parameter $K\mu_s(t_{stick})$ extracted from the fit of the maximum force F_{max} of this stick-slip event with Eq. (8). In the following, the results of this analysis for duralumin and brass columns are compared and discussed.

Steel/duralumin. For steel beads in the duralumin column, the parameter $K\mu_s$ [Figs. 16(b) and 17(b)] increases roughly logarithmically with aging time, and increases strongly with

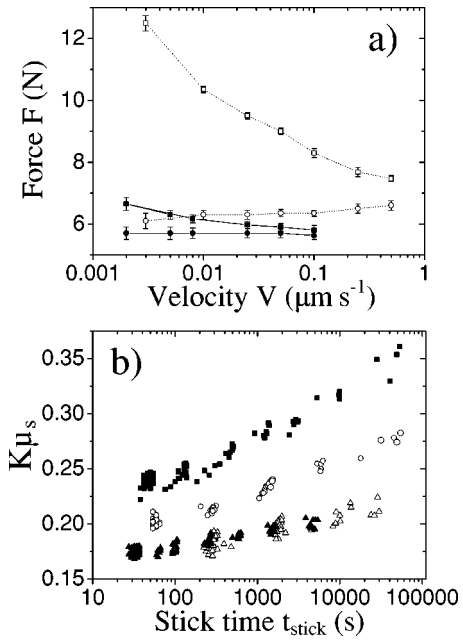

FIG. 18. (a) Minimum and maximum resistance forces F_{min} (circles) and F_{max} (squares) vs driving velocity in the stick-slip regime for a height $H=1.7D$ (300 g) of steel beads in the brass cylinder, for relative humidities $\chi=90\%$ (open symbols) and $\chi<3\%$ (filled symbols). (b) $K\mu_s$ as a function of stick time t_{stick} for a height $H=1.7D$ (300 g) of steel beads in the brass cylinder, for relative humidities $\chi=90\%$ (filled squares) and $\chi<3\%$ (filled triangles); and for a height $H=2.15D$ (380 g) for relative humidities $\chi=64\%$ (open circles) and $\chi<3\%$ (open triangles).

relative humidity χ. Its value increases by 50% when χ increases from 3% to 45%, and doubles when χ increases from 45% to 90%. The parameter $K\mu_s$ does not depend only globally on χ, but its logarithmic aging rate Kb with stick time t_{stick} depends strongly on χ. The values of parameter Kb extracted from a logarithmic fit of $K\mu_s(t)$, with $\mu_s(t)=\mu_0+b\ln(t/\tau_0)$, are given in Table III for different relative humidities.

Note that magnitude of Kb, as K is of the order 1, is consistent with many previous reports on solid friction [3,4]. An important feature is that the logarithmic aging rate appears to be four times higher in humid atmosphere than in dry atmosphere.

The logarithmic evolution is not perfect: for aging time larger than 3000 s, we observe that $K\mu_s$ increases more sharply with time; for $H=2.15D$ of steel beads and $\chi=45\%$, Kb varies from 0.009 for times $t_{stick}<3000$ s to about 0.025 in the last time decade [Fig. 17(b)]. This phenomenon was observed for all relative humidities χ. It is similar to what was reported previously by Losert and coworkers [9] for plane shearing of glass beads.

TABLE III. Parameter Kb extracted from a fit of $K\mu_s(t)$ with $\mu_s(t)=\mu_0+b\ln(t/\tau_0)$ for different relative humidities χ, for a height $H=1.4D$ (250 g) and a height $H=2.15D$ (380 g) of steel beads in the duralumin column.

Relative humidity χ (%)	Kb
<3	0.006 ± 0.001
45	0.013 ± 0.003
90	0.023 ± 0.001

TABLE IV. Parameter Kb extracted from a fit of $K\mu_s(t)$ with $\mu_s(t)=\mu_0+b\ln(t/\tau_0)$ for different relative humidities χ, for a height $H=1.7D$ (300 g) and a height $H=2.15D$ (380 g) of steel beads in the brass column.

Relative humidity χ (%)	Kb
<3	0.006 ± 0.001
64	0.011 ± 0.0005
90	0.014 ± 0.0005

It is tempting to link this enhanced aging behavior to the granular material's slow restructuring effects since one may think of an aging of the granular structure leading to a better stress redirection at the walls.

However, at this point, it is not possible to differentiate between wall and structure properties. We tried to measure independently μ_s aging properties in a solid-on-solid experiment, but we did not obtain satisfactory statistics to conclude. Therefore, we need to compare the results obtained in the duralumin column to the one obtained in the brass column.

Steel/brass. For steel beads in the brass column, the parameter $K\mu_s$ extracted from the experimental measurements [Fig. 18(b)] also increases logarithmically with aging time. However, the increase with relative humidity χ is much less important than in the duralumin column since the $K\mu_s$ increase is only 50% when increasing χ from dry atmosphere to 90% humidity, whereas the increase is more than 150% in the duralumin column for the same variation of χ. Moreover, the $K\mu_s$ increase with stick time seems now perfectly logarithmic over four decades of time variation.

As in the duralumin column, $K\mu_s$ increase rate with stick time t_{stick} depends on χ. The values of parameter Kb extracted from a logarithmic fit of $K\mu_s(t)$, with $\mu_s(t)=\mu_0+b\ln(t/\tau_0)$, are given in Table IV. Logarithmic aging rate is now 2.5 times greater in humid atmosphere than in dry atmosphere (it was four times higher in the duralumin column).

Comments. Since the only difference between both systems (duralumin and brass columns) is the contacts at the walls, as for the steady-sliding regime, the differences observed in the rheological behavior suggest that the aging of $K\mu_s$ is mainly an aging of friction coefficient μ_s at the walls and that humidity affects principally the contacts at the walls.

Relative humidity χ seems to have two effects in the duralumin column: first, the aging rate is higher when χ is higher, second, the friction level for short times is higher when χ is higher.

In the brass column there seems to be an effect of χ only on the aging rate: the $K\mu_s(t_{stick})$ curves for different χ cross for $t=0.1$ ms. The logarithmic aging rate coefficient gets comparable values in both columns, but it is higher in the

duralumin column ($Kb=0.023$) in humid atmosphere than in the brass column ($Kb=0.014$).

Our observations are consistent with recent aging experiments in granular media [6,7] and solid-on-solid aging experiments [4], where logarithmic aging of static friction enhanced by an increase in relative humidity χ was found. These results have been interpreted by the dynamics of capillary condensation at the contacts [6,8], which is a thermally activated process. As time goes on, there are more and more capillary bridges at the contacts, which are responsible for an adhesion force increasing with aging time; moreover, condensation goes faster when χ is higher. In these models, there is no aging in dry atmosphere, as no condensation can occur; this prediction agrees with most observations [4]. As in our experiment the logarithmic aging rate coefficient is not zero in dry atmosphere (even though the air flux we impose is probably not perfectly dry), we can conclude that capillary condensation is not the only source of aging. Another source of aging can be creep of contacts [3].

We observed that aging is perfectly logarithmic in the brass column. Therefore, we are led to analyze again the aging in the duralumin column since the interpretation based on aging of internal friction we proposed for the duralumin column should also apply to the brass column, which is in contradiction with the observed behavior.

If we assume that K properties depend only on the granular material properties, the acceleration of logarithmic aging in the duralumin column may be not linked to aging of bead-bead contacts or granular slow restructurations. We may then start from the following experimental observations: in solid-on-solid friction experiments, static friction coefficients μ_s are found to depend on the applied shear exerted for a given waiting time [3,30]. For a higher shear during a given waiting time, coefficient μ_s is higher and the logarithmic aging rate is higher too [3]. In our experiments, during a ''stick'' event, the pushing force increases linearly with time, i.e., shear at the walls (and contact pressure) increases. As a consequence, aging occurs with a nonconstant applied shear and the mean shear is more important when the aging time is higher. Consequently for high waiting time or stick time, i.e., for high mean shear at the walls, the aging of the static friction coefficient may be accelerated.

This phenomenology may be *a priori* different for different surfaces, which would explain why aging seems perfectly logarithmic in the brass column, and not in the duralumin column.

3. Analysis of F_{max} evolution

Now, the high enhancement of the blocking resistance force F_{max} with decreasing driving velocity can be simply understood within the Janssen framework. We start from the experimental observation that the minimum force F_{min} after a slip does not depend on velocity (at constant relative humidity χ): $F_{min}=F_0$. Therefore, the aging time t_{stick} before a slip reads

$$t_{stick}=(F_{max}-F_0)/(kV). \tag{9}$$

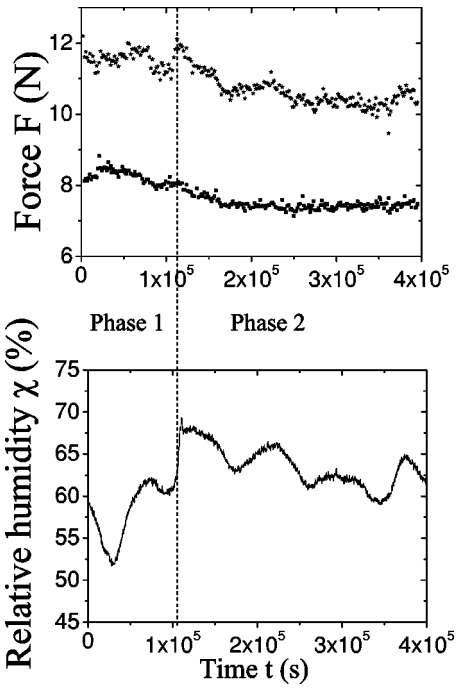

FIG. 19. (a) Maximum and minimum resistance forces to pushing F_{max} (stars) and F_{min} (squares) of a height $H=2.15D$ (380 g) of steel beads in the duralumin cylinder vs time in the stick-slip regime ($V=50$ nm s^{-1}). (b) Evolution of relative humidity χ during the experiment of (a). The dotted line separates two phases: (1) forces and χ evolutions are not correlated; (2) forces and χ evolutions are correlated.

We suppose, as well-verified experimentally, that the coefficient of friction μ_s at the walls follows a logarithmic aging law:

$$\mu_s(t)=\mu_0+b\ln(t/\tau). \tag{10}$$

This value of $\mu_s(t)$ for aging time t_{stick} can be injected in formula (8). We then obtain

$$F_{max}\propto V^{-1/\gamma} \tag{11}$$

with $\gamma=R/(2KbH)-1$.

The apparent divergence of F_{max} with decreasing velocity, as observed experimentally, is thus more important when the height of beads and the logarithmic aging rate b of friction at the walls (i.e., relative humidity as b increases with χ) are higher. The observed strong dependence of F_{max} with V then corresponds to an exponential amplification of friction aging at the walls. Elements of interpretation along these lines were already given in Ref. [16].

C. Influence of relative humidity: An open problem

Nevertheless from the whole series of experiments we performed on this system, we are led to conclude that the dependence of the phenomenology with the relative humidity χ remains sometimes unclear.

As an illustration of this statement, we report the following result (Figs. 19 and 20). In an experiment performed in

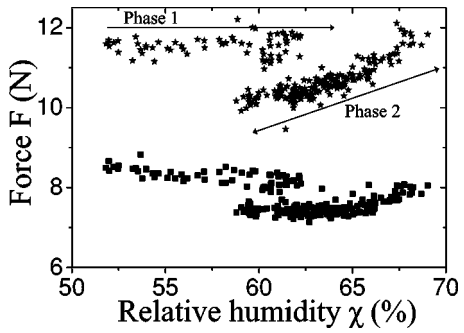

FIG. 20. Maximum and minimum forces F_{max} (stars) and F_{min} (squares) vs relative humidity χ for the experiment of Fig. 19; phases (1) and (2) of Fig. 19 are indicated on the graph.

the stick-slip regime and in the ambient atmosphere, for a driving velocity $V=50\ \mathrm{nm\,s^{-1}}$, the forces F_{min} and F_{max} were found to be independent of χ, which was varying between 52% and 62%, during the first 30 h of the experiment. We then observed that the F_{min} and F_{max} variations became suddenly correlated to the χ variations and would stay correlated for the next 80 h. For the first 30 h, χ increased from 52% to 62%, while F_{min} and F_{max} were nearly constant: $F_{max}=11.6$ N, $F_{min}=8.2$ N. Then χ varied from 62% to 68% in 1 h: F_{min} and F_{max} started to be correlated to χ from this ''triggering event'' and for the next 80 h as if the system had suddenly reached some ''reversible branch.''

Such a phenomenology was never obtained when humidities $\chi=90\%$ and $\chi<3\%$ were imposed. When we imposed dry atmosphere, the force would reach its stationary value in a few minutes and we never noticed any variation in this value for 5 days; when we imposed humid atmosphere, the force would reach its stationary value in a maximum of 3 h and we noticed no variation in this value for 5 days.

This may, however, incite to prudence for results obtained in the ambient atmosphere, for experiments performed on the granular column as much as for solid-on-solid friction experiments. As an example, we see in Fig. 20 that for $\chi=60\%$, $F_{max}=11.5\pm0.2$ N when forces and χ are not correlated, whereas $F_{max}=10.3\pm0.2$ N when they are correlated.

Furthermore, this opens the question of the metastability of capillary condensation. If variation of F_{max} with χ is interpreted as variation of μ_s due to thermally activated capillary condensation at the contacts [6,8], it seems possible that capillary condensation did not occur for hours. If we note that F_{max} starts to be correlated with χ when constant value of F_{max} is equal to F_{max} on the χ dependent part of the curve (i.e., $F_{max}=11.8$ N and $\chi=68\%$), another possibility is that there were as much capillary bridges condensed at the contacts as for $\chi=68\%$ in the first part of the experiment, i.e., evaporation does not always happen.

D. Dieterich-Ruina analysis

A standard phenomenological model accounting for static and dynamic properties of solid friction is the so-called Dieterich-Ruina model [27,28]. In this picture, the coefficient of friction is

$$\mu=\mu_0+a\ln\left(\frac{V}{V_0}\right)+b\ln\frac{V_0\theta}{D}, \tag{12}$$

where θ obeys [31]

$$\frac{d\theta}{dt}=1-\frac{\theta V}{D}; \tag{13}$$

μ_0, a, b, and D are constants dependent on the materials in contact. Parameter D is usually interpreted as a characteristic length for renewal of contacts and is of the order of the creep length before sliding [10]. In a stationary steady-sliding regime, $\theta=D/V$ is interpreted as a characteristic time for renewal of contacts.

This model accounts for the logarithmic aging of static friction, and the logarithmic velocity strengthening or weakening in the steady-sliding regime with

$$d\mu_s/d\ln(t)=b, \tag{14}$$

$$d\mu_d/d\ln(V)=a-b. \tag{15}$$

It also accounts for a third usual phenomenon observed in the transitory regime when the velocity is changed suddenly. In this case there is an abrupt change in friction coefficient followed by exponential relaxation to a new stationary value. If we change velocity V_1 to velocity V_2, the instantaneous change in friction coefficient from stationary value $\mu_d(V_1)=\mu_0+(a-b)\ln(V_1/V_0)$ is $+a\ln(V_2/V_1)$; friction change from this value to new stationary value $\mu_d(V_2)$ is then $-b\ln(V_2/V_1)$ during typical time $\tau=D/V_2$, i.e., we get $\mu_d(V_2)=\mu_0+(a-b)\ln(V_2/V_0)$.

Now we test the Dieterich-Ruina model with the steel/duralumin and steel/brass friction coefficient extracted from our data. As we observed logarithmic aging and rough logarithmic velocity strengthening, we get parameters a and b. We are therefore able to test this model predictions with the observation of response to an abrupt variation of velocity.

Experimentally, we never observed any transitory state: the force in the steady-sliding regime was always changed from stationary value $\overline{F}(V_1)$ to stationary value $\overline{F}(V_2)$ when changing velocity from V_1 to V_2. From the measured value of $Kb=0.010$ for steel/duralumin friction and $Kb=0.011$ for steel/brass in the ambient atmosphere, we would, however, expect the force at the beginning of the transitory regime to be 0.5 N larger (steel beads height $H=2.15D$) than the stationary force at the new velocity. As the natural fluctuations of force are around 0.1 N, we would therefore expect to observe this transitory regime in $\overline{F}$ due to change in friction at the walls. Now we give an interpretation for why, within the Dietrich-Ruina picture, this transitory regime was not observed, which yields an upper bound for the material contact renewal length D_0.

When velocity is changed from $10\ \mu\mathrm{m\,s^{-1}}$ to $100\ \mu\mathrm{m\,s^{-1}}$ for $H=2.15D$ (380 g) of steel beads in a duralumin cylinder, the change in the $\overline{F}$ stationary value is of 1 N. But, due to the finite stiffness of our setup, this change cannot be instantaneous: an increase ΔF of force at constant velocity takes minimal time $t=\Delta F/(kV)$. So an increase of

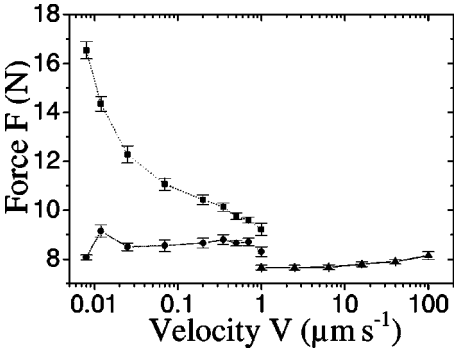

FIG. 21. Mean maximum and minimum forces F_{max} (squares, dotted line) and F_{min} (circles, dashed line) in the stick-slip regime, and mean resistance force $\overline{F}$ (triangles, full line) in the steady-sliding regime for a height $H=2.15D$ (380 g) of steel beads in the duralumin cylinder, for relative humidity $\chi=40\%$.

1 N of force at 100 μm s^{-1} takes time $t=0.25$ s. This time must be compared to time length τ of transitory regime: $\tau=D_0/V$. Therefore, in the framework of the Dieterich-Ruina model, we need τ to be less than the time of force variation, which means $D_0<25$ μm .

Let us now consider a sudden decrease in velocity from 100 μm s^{-1} to 1 μm s^{-1}. Now the decrease of force is governed by inertial time: $t_{in}=\pi\sqrt{m/k}$, which can be evaluated around $t_{in}=200$ ms. This leads to $D_0<400$ nm (so that $\tau<t_{in}$) consistently with the Dieterich-Ruina model if no transitory state is observed.

We have no precise measure for D_0 but this upper limit on the value is coherent with the usual interpretation in terms of length for contact renewal, as the duralumin column mean roughness is 400 nm. Thus, we can neither validate nor rule out the Dieterich-Ruina model for our system.

E. Transition mechanism

For experiments performed at given height of beads and relative humidity χ, we observe that the transition from stick slip to steady sliding occurs for a finite stick-slip amplitude (Fig. 21). This suggests a subcritical transition but such a transition would be hysteretic. In order to verify this feature, we make the following experiment: we drive the system at a constant velocity in the steady-sliding regime near the transition until it reaches a stationary state, we then decrease continuously the velocity, without ever stopping the movement, to a velocity for which stick slip used to occur. Note that the results reported in the previous sections and in Fig. 21 were obtained for independent experiments on systems driven at a unique velocity. We observe that if we impose $V=700$ nm s^{-1} directly, we obtain a stick-slip motion, whereas when we decrease velocity from 1.4 μm s^{-1} (in the steady sliding regime) to $V=700$ nm s^{-1} the motion is steady sliding. This proves the hysteretic character of the transition, which was actually hard to observe as the system seems very sensitive to noise.

This transition is similar to the one observed by Heslot *et al.* [10] in solid-on-solid experiments; it corresponds to what they call the ''inertial regime.'' It is a characteristic of systems for which the dynamical coefficient of friction increases with velocity. This transition scenario was explained by Brockley *et al.* [32]. However, they found that the force $\overline{F}$ in the steady-sliding regime at the transition is of order of F_{min}. We actually find (see Fig. 21) that $\overline{F}$ is less than F_{min} for steel beads in the duralumin cylinder, a feature we do not understand, whereas $\overline{F}\approx F_{min}$ in the brass cylinder.

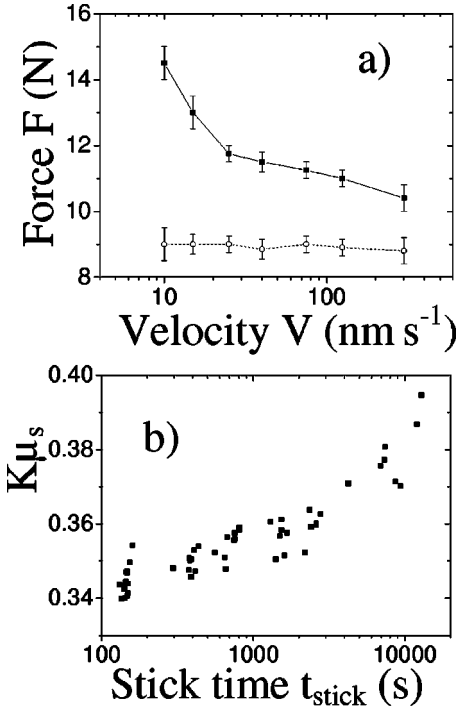

FIG. 22. (a) Minimum and maximum resistance forces F_{min} (open circles) and F_{max} (full squares) vs driving velocity in the stick-slip regime for a height $H=2.8D$ (132 g) of a miscellany of glass beads in the PMMA cylinder at relative humidity $\chi=35\%$. (b) $K\mu_s$ as a function of stick time t_{stick} extracted from F_{max} with Eq. (8).

Again, the transition we observed is consistent with a picture of solid friction sliding instability at the wall. This is also consistent with the model we have developed in the preceding section.

IV. POLYDISPERSE GLASS BEADS

After the study of the simplest case, with monodisperse low friction beads, we now want to study the effect of disorder (friction, polydispersity) on rheology. Therefore, we choose to study a miscellany of glass beads using a mixture of three diameters (1.5 mm, 2 mm, and 3 mm) with equal volume of each kind in an abraded PMMA cylinder. In the following, we present the features obtained in the stick-slip regime for this system.

A. Stick-slip characterization

For low velocities ($V<100$ nm s^{-1}), a stick-slip motion is obtained with the same properties as observed with monodisperse steel beads in a duralumin or brass cylinder. It is a

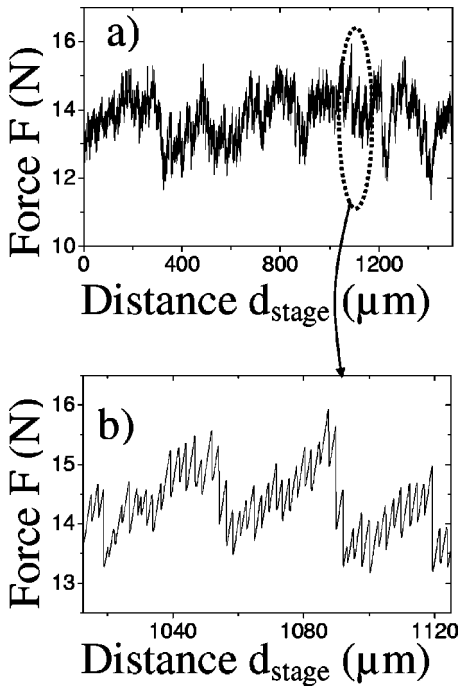

FIG. 23. (a) Resistance force to pushing of a height $H=2.7D$ (126 g) of a miscellany of glass beads in the PMMA cylinder vs displacement d_{stage} of the translation stage in the stick-slip regime ($V=1500$ nm s^{-1}); (b) zoom of (a).

regular stick-slip motion characterized by a maximum force before slipping that increases strongly when velocity is decreased and a minimum force after slipping which does not depend on velocity [Fig. 22(a)]. A coefficient $K\mu_s(t_{stick})$ can be extracted from F_{max} with Eq. (8) for low velocities ($V<100$ nm s^{-1}). Again, it shows a logarithmic aging of friction at the walls [Fig. 22(b)]. However, the behavior changes for higher velocities just before the transition to steady sliding. The stick-slip motion is then less and less regular as the velocity is increased. Furthermore, we observe structures in the force signal. Figure 23 evidences cycles of force increase during which the maximum and minimum forces increase for several stick-slip events, as the force amplitude ΔF_{stick} during a stick is higher than the force amplitude ΔF_{slip} during a slip. Then, at the end of a cycle, there is a big slip event and a new cycle starts. This phenomenon is similar to the one observed by Albert *et al.* [12] for the pushing of a stick in a granular material and to the one observed for aluminum beads by Kolb *et al.* [15] in the same display as ours but in 2D. It was, however, much more important in that study in 2D: the force F_{max} would then increase from 2 N after a big slip event to 20 N before the next big slip event.

We analyze this phenomenon by studying the distribution of force amplitudes defined as $\Delta F_{stick}=F_{max}(i)-F_{min}(i)$ for the ith stick event, and $\Delta F_{slip}=F_{max}(i)-F_{min}(i+1)$ for the following slip event (Fig. 24). We observe the evolution of these distributions with increasing velocity. ΔF_{stick} distribution remains centered around a mean value; however, this distribution gets larger when the velocity is increased. For lower velocities [150 nm s^{-1} in Fig. 24(a)], stick slip is regular and ΔF_{slip} distribution is regular around same mean

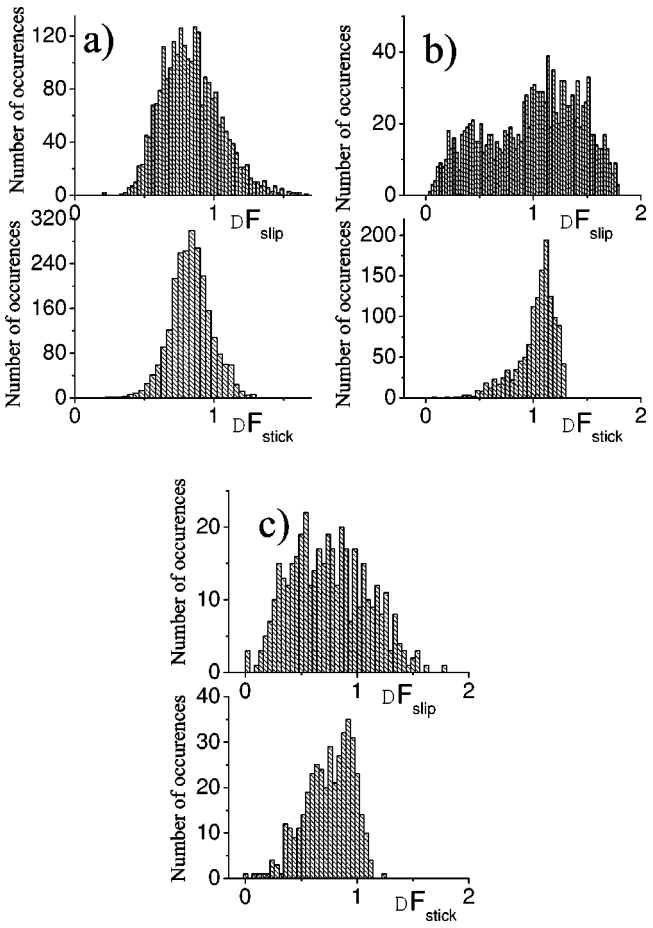

FIG. 24. Distribution of force variations $\Delta F_{stick}=F_{max}(i)-F_{min}(i)$ during a stick and $\Delta F_{slip}=F_{max}(i)-F_{min}(i+1)$ during a slip of a height $H=2.7D$ (126 g) of a miscellany of glass beads in the PMMA cylinder for three driving velocities: (a) $V=150$ nm s^{-1}; (b) $V=750$ nm s^{-1}; (c) $V=1500$ nm s^{-1}.

value as ΔF_{stick} (with nevertheless a larger distribution). When velocity is increased, the distribution is still predominant around same mean value as ΔF_{stick} but many smaller values start to merge in the distribution [$V=750$ nm s^{-1} in Fig. 24(b)]; these small values become as frequent as the larger ones for higher velocities [$V=1500$ nm s^{-1} in Fig. 24(c)]. The distribution also enlarges to the higher values which corresponds to occurrence of the big slip events. Note that in these experiments, the transition to steady-sliding regime occurs for a velocity around $V=2000$ nm s^{-1}.

B. Analysis

Several explanations can be proposed to account for this complex dynamics exhibiting a large distribution of energy release. In our point of view, the principal ingredient for an explanation seems to be the progressive structuration of the packing between two big slip events. In the Janssen model picture, the progressive increase of F_{max} in a cycle corresponds to progressive increase of Janssen's constant K. The K value increases from an initial value K_0 at the beginning of a cycle up to a maximum value K_{max} at the end of the cycle, and is reinitialized by a big slip event to value K_0. Let us

recall that K was found to increase with density in another paper [19]. A consequence of this dependence was shown in Sec. III A 1. Therefore, a way to obtain the phenomenology is to start from a loose packing at the beginning of a cycle. If each small slip event densifies the packing (as can be expected from compaction under vibration), it leads to a small increase in K, so that the minimum force F_{min} at the end of the slip is higher than the force F_{min} at the end of the preceding slip; the maximum force F_{max} at the end of the stick is also higher than the force F_{max} at the end of the preceding stick. Sometimes, big events occur; they probably correspond to convective motion at the walls (as observed by Kolb *et al.* in 2D [15]) which loosens the packing, which then gets the initial density of the cycle.

Within the interpretation we give, the stick events last a constant time as the aging time of contacts at the walls is still controlled by the velocity. This explains why the distribution of ΔF_{stick} is still centered on mean value contrary to ΔF_{slip}.

But still a criterion for big slip events has yet to be found; it may be the level of stresses or a dilatancy effect at high density causing shear band and convection rolls. The regularity of stick-slip motion at low velocities can be understood if the criterion for big slip events is at an upper stress level. A slow driving velocity leads to long aging of contacts at the walls so that the maximum force F_{max} is always greater than the threshold to obtain a big slip. All slip events are then big slip events in this case.

This transition from a simple steady stick slip to a complex dynamical regime with a large distribution of elastic energy release is an interesting issue and we plan to pursue further the investigation trying to clarify in particular the role of disorder and polydispersity in the phenomenology.

V. CONCLUSION

We presented an experimental report on the dynamical behavior of a granular column pushed vertically. The wall roughness of the cylindrical container is much smaller than the typical grain size. We first investigated the case of a monodisperse assembly of steel beads and observed at low driving velocities ($1<V<100$ μm/s) a steady behavior such that the pushing forces increase roughly logarithmically with velocity. On the other hand, at very low driving velocity ($V<1$ μm/s), we evidenced a discontinuous and hysteretic transition to a stick-slip regime characterized by a strong divergence of the maximal blockage force when the velocity goes to zero. All this phenomenology is strongly influenced by surrounding humidity: generally, higher humidity level increases strongly the resistance to pushing. Finite element numerical simulations were used to confront experimental results to a modeling of the granular packing as an isotropic elastic medium. Then, we showed that a simple Janssen's model is a fair base for analysis as it provides the correct physical interpretation for the pushing resistance. This Janssen's model was used to extract an important mechanical parameter combining the effects of stress redirection and wall friction, but there is an inherent difficulty to isolate clearly the various contributions either coming from bulk reorganization or from the surface friction properties.

Using different column materials and measuring directly the friction of a grain with the wall, we accumulated several evidences leading us to conclude that the force dependence with driving velocity and humidity is strongly related to the bead-wall friction properties: (i) in the steady limit grain/wall tribology measurements show a friction force increasing with humidity and velocity; (ii) in the stick-slip regime, the blockage enhancement can be related to humidity induced aging of the bead-wall friction; (iii) the hysteretic transition mechanism from stick slip to steady sliding is similar to the one observed in solid-on-solid experiments [32,10].

In spite of a dominant surface effect, we could also identify contributions of bulk structurations. For example, we related the transitory part of the response to pushing to a dependence of the coefficient of redirection between horizontal and vertical stress with packing fraction. Also, a clear difference of the mechanical parameters extracted from pushing and pulling experiments shows a contribution of texturation effects of about 20%.

A second system, made of polydisperse assemblies of glass beads, was investigated. We emphasize the onset of a new complex dynamical behavior, i.e., the large distribution of blockage forces evidenced in the stick-slip regime close to the transition.

ACKNOWLEDGMENTS

We acknowledge collaboration with C. Fond and E. Kolb. We thank C. Gauthier for his kind hospitality at the ICS in Strasbourg and his valuable comments on tribology. We thank J. Lanuza and P. Lepert for technical support. We are grateful to Professor T. Baumberger, Professor R. P. Behringer, and Professor C. Caroli for many interesting discussions.

[1] *Physics of Dry Granular Media*, edited by H.J. Herrmann, J.-P. Hovi, and S. Luding (Kluwer Academic Dordrecht, 1998); E. Clément, Curr. Opin. Colloid Interface Sci. **4**, 294 (1999).
[2] D.M. Wood, *Soil Behaviour and Critical State Soil Mechanics* (Cambridge University, Cambridge, UK, 1990).
[3] P. Berthoud *et al.*, Phys. Rev. B **59**, 14313 (1999).
[4] J. Crassous *et al.*, Europhys. Lett. **47**, 562 (1999).
[5] E. Riedo, F. Lévy, and H. Brune, Phys. Rev. Lett. **88**, 185505 (2002).
[6] L. Bocquet *et al.*, Nature (London) **396**, 735 (1998).
[7] F. Restagno, H. Gayvallet, and E. Charlaix, Phys. Rev. E **66**, 021304 (2002).
[8] F. Restagno *et al.*, J. Phys.: Condens. Matter **12**, A419 (2000).
[9] S. Nasuno, A. Kudrolli, and J.P. Gollub, Phys. Rev. Lett. **79**, 949 (1997); J.C. Géminard, W. Losert, and J.P. Gollub, Phys. Rev. E **59**, 5881 (1999); W. Losert *et al.*, *ibid.* **61**, 4060 (2000).
[10] F. Heslot *et al.*, Phys. Rev. E **49**, 4973 (1994).
[11] V.K. Horvath, I.M. Janosi, and P.J. Vella, Phys. Rev. E **54**, 2005 (1996).
[12] R. Albert *et al.*, Phys. Rev. Lett. **82**, 205 (1999); G. D'Anna,

Europhys. Lett. **51**, 293 (2000).
[13] M. Lubert and A. de Ryck, Phys. Rev. E **63**, 021502 (2001).
[14] J.-L. Aider *et al.*, Phys. Rev. E **59**, 778 (1999).
[15] E. Kolb *et al.*, Eur. Phys. J. B **8**, 483 (1999).
[16] G. Ovarlez, E. Kolb, and E. Clément, Phys. Rev. E **64**, 060302 (2001).
[17] Y. Bertho, F. Giorgiutti-Dauphine, and J.-P. Hulin, Phys. Rev. Lett. **90**, 144301 (2003).
[18] J.W. Landry *et al.*, Phys. Rev. E **67**, 041303 (2003).
[19] G. Ovarlez, C. Fond, and E. Clément, Phys. Rev. E **67**, 060302(R) (2003).
[20] G. Ovarlez, C. Fond, and E. Clément (unpublished).
[21] The surface topogaphy was obtained at the Institut Charles Sadron in Strasbourg with Christian Gauthier.
[22] O. Pouliquen, M. Nicolas, and P.D. Weidman, Phys. Rev. Lett. **79**, 3640 (1997).
[23] R. Ben Aïm and P. Le Goff, Powder Technol. **1**, 281 (1967).
[24] L. Vanel, Ph.D. thesis, University of Paris VI, 1999.
[25] L. Vanel and E. Clément, Eur. Phys. J. B **11**, 525 (1999).
[26] See, http://www.castem. org:8001
[27] J.H. Dieterich, J. Geophys. Res. **84**, 2161 (1979).
[28] A. Ruina, J. Geophys. Res. **88**, 359 (1983).
[29] T. Baumberger, Solid State Commun. **102**, 175 (1997).
[30] G. Ovarlez, C. Gauthier, and E. Clément (private communication).
[31] There are other models for θ, some of them are recessed by Ruina [28].
[32] C.A. Brockley, R. Cameron, and A.F. Potter, J. Lubr. Technol. **89**, 101 (1967).